Tanaka-Tagoshi parametrization of post-first-post-Newtonian spin-free gravitational wave chirps: Equispaced and cardinal interpolated lattices for first generation interferometric antennas

R. P. Croce and Th. Demma

Wavesgroup, Dipartimento di Ingegneria dell' Informazione e Ingegneria Elettrica, University of Salerno,
Via Ponte don Melillo, 1, 84084 Fisciano (SA), Italy

V. Pierro and I. M. Pinto

Wavesgroup, University of Sannio at Benevento, Piazza Roma, Pal. Bosco Lucarelli, 82100 Benevento, Italy

The spin-free binary-inspiral parameter-space introduced by Tanaka and Tagoshi to construct a uniformly spaced lattice of post-first-post Newtonian (PN) templates is shown to work for all first generation interferometric gravitational wave antennas. This allows us to extend the minimum-redundant cardinal interpolation techniques of the correlator bank developed by the authors to the highest available order PN templates. The total number of templates to be computed for a minimal match $\Gamma = 0.97$ is reduced by a factor 4, as in the 1PN case.

I. INTRODUCTION

Gravitational waves emitted by coalescing compact binaries in their adiabatic inspiral phase have been accurately modeled [1] and are preferred candidates for the direct detection of gravitational radiation of cosmic origin, by the first generation of broadband laser interferometric antennas, including TAMA300 [2], GEO600 [3], the Laser Interferometric Gravitational Wave Observatory (LIGO) [4], and VIRGO [5].

The best strategy for detecting signals of known form in colored Gaussian stationary noise consists in correlating the detector output (data) with a discrete family (lattice) of expected wave forms (templates), and using the largest correlation as a detection statistic (maximum likelihood [6]). The above correlation is the (weighted) scalar product

$$\langle a,g \rangle \equiv 2 \left[\int_{f_i}^{f_s} a(f) g^*(f) \frac{df}{\Pi(f)} + \text{c.c.} \right], \qquad (1.1)$$

where (f_i, f_s) is the antenna spectral window, $a(f) = h(f) + n(f)$ are the (noise-corrupted, spectral) data, $h(f)$ is a (possibly null) signal and $n(f)$ a realization of the antenna noise, $g(f)$ is a template, $\Pi(f)$ is the (one-sided) antenna noise power spectral density, and c.c. denotes the complex conjugate. The detection statistic has to be compared to a threshold, which depends on the allowed false alarm probability. At any fixed false-alarm probability, the largest probability of detection is obtained if a template is exactly *matched* to the signal. The matching between h and g is measured by their *overlap*,

$$\mathcal{O}(h,g) = \frac{\langle h,g \rangle}{||h|| \cdot ||g||} \leq 1, \qquad (1.2)$$

where the norm $||u|| = \langle u,u \rangle^{1/2}$. The template lattice should be designed in such a way that for *any* admissible signal, one can always find *at least one* template in the lattice such that [7] the overlap is never less than a prescribed Γ.

In the straightforward restricted [8] post-Newtonian (PN) stationary-phase approximation [9] the spectral form of a null-eccentricity binary inspiral signal is

$$h(f) = A f^{-7/6} \exp\{j[2\pi f T_c - \phi_c + \Psi^{(\nu)}(f,\vec{\xi}) - \pi/4]\}, \qquad (1.3)$$

where A is a (real, unknown) constant, depending on the source position, T_c is the fiducial coalescency time [10], ϕ_c is the phase at $t = T_c$, and [11]

$$\Psi^{(\nu)}(f,\vec{\xi}) = \sum_{i=1}^{2\nu+1} \zeta_i(f) \theta^i(\vec{\xi}), \qquad (1.4)$$

where ν is the PN order, and $\vec{\xi}$ represents the remaining (intrinsic) source parameters. The functions ζ_i and θ^i are presently known up to 2.5PN order [12] and are collected in Table I [13] in terms of the intrinsic parameters m (total mass of the binary), $\eta = \mu/m$ (μ being the reduced mass), β and σ (spin-orbit and spin-spin terms, respectively [14]).

Maximizing explicitly the overlap over the (irrelevant, *extrinsic*) parameters $\Delta\phi_c$ and ΔT_c, one can write the template-lattice design prescription as

$$\forall h \in \mathcal{S}, \ \exists g \in \mathcal{L}: \ M(h,g) \equiv \sup_{\Delta T_c} \frac{\left| \int_{f_i}^{f_s} f^{-7/3} \exp\{j[2\pi f \Delta T_c + \Delta\Psi^{(\nu)}(f,\vec{\xi}_h,\vec{\xi}_g)t]\} \frac{df}{\Pi(f)} \right|}{\int_{f_i}^{f_s} f^{-7/3} \frac{df}{\Pi(f)}} \geq \Gamma, \qquad (1.5)$$

TABLE I. Relevant to Eq. (1.4).

PN order	i	$\zeta_i(f)$	θ^i
0	1	$\left(\dfrac{f}{f_0}\right)^{-5/3}$	$\dfrac{3}{128\eta}(\pi m f_0)^{-5/3}$
0.5	2	$\left(\dfrac{f}{f_0}\right)^{-4/3}$	0
1	3	$\left(\dfrac{f}{f_0}\right)^{-1}$	$\dfrac{5}{96\eta}\left(\dfrac{743}{336}+\dfrac{11}{4}\eta\right)(\pi m f_0)^{-1}$
1.5	4	$\left(\dfrac{f}{f_0}\right)^{-2/3}$	$\dfrac{3}{32\eta}(\beta-4\pi)(\pi m f_0)^{-2/3}$
2	5	$\left(\dfrac{f}{f_0}\right)^{-1/3}$	$\dfrac{15}{64\eta}\left(\dfrac{3058673}{1016064}+\dfrac{5429}{1008}\eta+\dfrac{617}{144}\eta^2-\sigma\right)(\pi m f_0)^{-1/3}$
2.5	6	$\log\left(\dfrac{f}{f_0}\right)$	$\dfrac{\pi}{128\eta}\left(\dfrac{38645}{252}+5\eta\right)$

where the partially maximized overlap $M(f,g)$ is called the *match*, $\mathcal{S}$ and $\mathcal{L}$ are the signal space and template lattice, respectively, and

$$\Delta\Psi^{(\nu)}(f;\vec{\xi}_h,\vec{\xi}_g)=\Psi^{(\nu)}(f,\vec{\xi}_h)-\Psi^{(\nu)}(f,\vec{\xi}_g)$$

$$=\sum_{i=1}^{2\nu+1}\zeta_i(f)[\theta^i(\vec{\xi}_h)-\theta^i(\vec{\xi}_g)]. \quad (1.6)$$

Whenever the match is only a function of the signal/template parameter *differences*, the template lattice is *uniform*, i.e., the lattice spacing is *constant* throughout the template parameter space, and depends uniquely on Γ [15]. This is obviously the case iff the function $\Delta\Psi^{(\nu)}$ depends, in turn, on the signal or template parameter differences only.

Uniformity is a key property for efficient implementation of the lattice. In a uniform lattice, templates corresponding to adjacent nodes differ only by a *constant* phase factor, which makes the template family construction computationally inexpensive. Furthermore, in view of the quasi-band-limited nature of the match as a function of the signal/template parameter differences, cardinal interpolation among the correlators can be used as shown in Refs. [16] and [17] to substantially reduce the number of templates required for a prescribed Γ.

The one-dimensional (1D) Newtonian ($\nu=0$) and 2D first-order post-Newtonian ($\nu=1$) wave forms can be easily parametrized so as to make the phase difference (1.6) a function of the signal/template parameter *differences* only [18]. On the other hand, according to present understanding, in order to keep $\Gamma\gtrsim0.97$ when working with *true* data, 2PN (or higher) templates will be needed, although spin-free ones should be adequate (see Sec. III A of [15]).

In the following we shall refer to 2PN templates. These are the best available ones for the purpose of detection/estimation. Indeed, as shown in [19], 2.5PN templates yield generally poorer overlaps (and larger biases) with (exact) numerically generated wave forms as compared to 2PN, as an effect of the peculiar (oscillating) behavior of PN-approximant sequences.

Unfortunately, at PN orders $\nu>1$, as shown in Sec. II, it is *strictly impossible* to parametrize the spin-free wave forms so as to make the phase difference (1.6) a function of the signal/template parameter *differences* only. As a result, the choice of template placement and spacing becomes, in principle, rather unwieldy, and the cardinal interpolation techniques discussed in Refs. [16] and [17] cannot be applied in any straightforward fashion.

Recently, Tanaka and Tagoshi [20] suggested a clever way to circumvent this difficulty, using a simple and elegant geometric argument yielding a uniform post-1PN template lattice. The scope of this paper is to illustrate the effectiveness of the Tanaka-Tagoshi construction for *all* first generation interferometers (TAMA300, GEO600, LIGO-I, and VIRGO) under a given minimal match constraint (see Sec. III), opening the possibility of using the minimum redundant cardinal interpolation of the correlator bank introduced and discussed in Refs. [16] and [17] with the highest available PN order templates. In the following we use geometrized units ($G=c=1$) throughout.

II. THE INTRINSIC CURVATURE OF THE SPIN-FREE PARAMETER SPACE MANIFOLD

The Tanaka-Tagoshi construction is best understood in the geometric language first introduced in Ref. [21]. The match between h and g can be accordingly written [22]:

$$M(h,g)=1-G_{rs}\Delta\theta^r\Delta\theta^s+\cdots, \quad (2.1)$$

where $\Delta\theta^i=\theta^i(\vec{\xi}_h)-\theta^i(\vec{\xi}_g)$, and the $(2\nu+1)$-dimensional metric G_{rs} is defined in Appendix A.

Let $m_{min}\leq m_1\leq m_2\leq m_{max}$ the spin-free wave form parameter space, m_1, m_2 being the companion masses [23]. In the $(2\nu+1)$-dimensional PN space θ^i the parameter space is
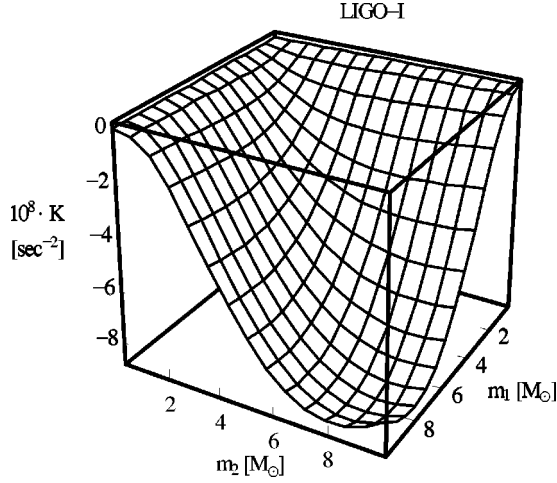
FIG. 1. The Gaussian curvature K of $\mathcal{P}$ vs m_1, m_2 for LIGO-I.

FIG. 2. The Gaussian curvature K of $\mathcal{P}$ vs $m_1 = m_2$ (worst case) for TAMA300, GEO600, LIGO-I, and VIRGO.

mapped into a three-vertex 2D manifold $\mathcal{P}$. Exploiting the dependence of θ^i on m_1 and m_2 one can rewrite Eq. (2.1) as

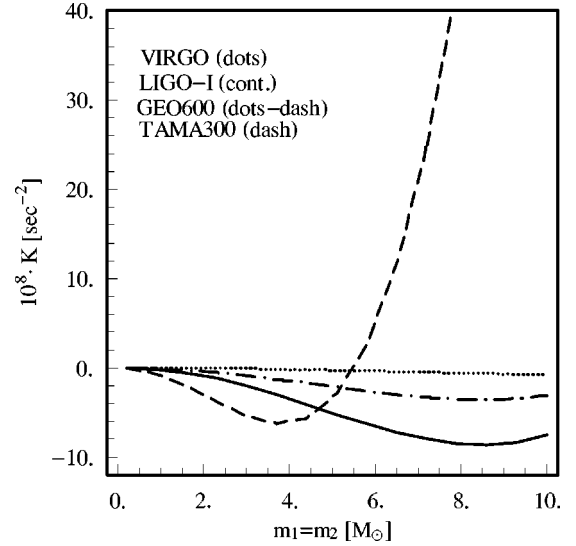$$M(h,g) = 1 - ds^2, \quad ds^2 = g_{pq}\Delta m^q \Delta m^p, \quad (2.2)$$

where

$$g_{pq} = G_{rs}\frac{\partial \theta^r}{\partial m_p}\frac{\partial \theta^s}{\partial m_q}, \quad (2.3)$$

is a 2D Finsler metric [24] on $\mathcal{P}$.

In order to find a chirp wave form parametrization which makes the match a function of the source-template *parameter differences* only, one should be able to find a coordinate transformation $(m_1, m_2) \rightarrow (x_1, x_2)$ such that

$$M(h,g) = 1 - \delta_{pq}\Delta x^p \Delta x^q, \quad (2.4)$$

where δ_{pq} is the 2D Euclidean metric. As anticipated, the required coordinate transformation does *not* exist, in general. This is due to the fact that the manifold $\mathcal{P}$ is *not* globally flat, as can be seen synthetically from its Gaussian curvature K [25]. The Gaussian curvature of $\mathcal{P}$ as a function of m_1, m_2 in $0.2 M_\odot \leq m_{1,2} \leq 10 M_\odot$ is shown in Fig. 1, for the special case of LIGO-I at 2PN order. The absolute curvature is maximum

for $m_1 = m_2$. This property turns out to be common to *all* first-generation antennas, whose relevant parameters have been collected in Table II. In Fig. 2 the curvature of $\mathcal{P}$ is displayed as a function of $m_1 = m_2$ (worst case) for TAMA300, GEO600, LIGO-I, and VIRGO at 2PN order.

III. THE TANAKA-TAGOSHI COORDINATES

Even though $\mathcal{P}$ is *not* flat, following Tanaka and Tagoshi it is still possible to place the templates on a *flat* manifold chosen *close* to $\mathcal{P}$ in a suitable sense. The Tanaka-Tagoshi construction can be simply phrased as follows: (i) introduce a linear coordinate transformation $\vec{\theta} \rightarrow \vec{x}$ such that *all three* vertices of the manifold $\mathcal{P}$ are brought onto the (x_1, x_2) plane of the (orthogonal) coordinate system x_i (see Appendix B for details), and then (ii) take the resulting three-vertex *flat 2D simplex* $\mathcal{T}$ in the (x_1, x_2) plane as the signal/template parameter space.

The flat simplexes $\mathcal{T}$ corresponding to $0.2 M_\odot \leq m_1 \leq m_2 \leq 10 M_\odot$ are shown in Fig. 3 for TAMA300, GEO600,

TABLE II. Spectral windows and noise power spectral densities of first generation interferometric GW antennas [15].

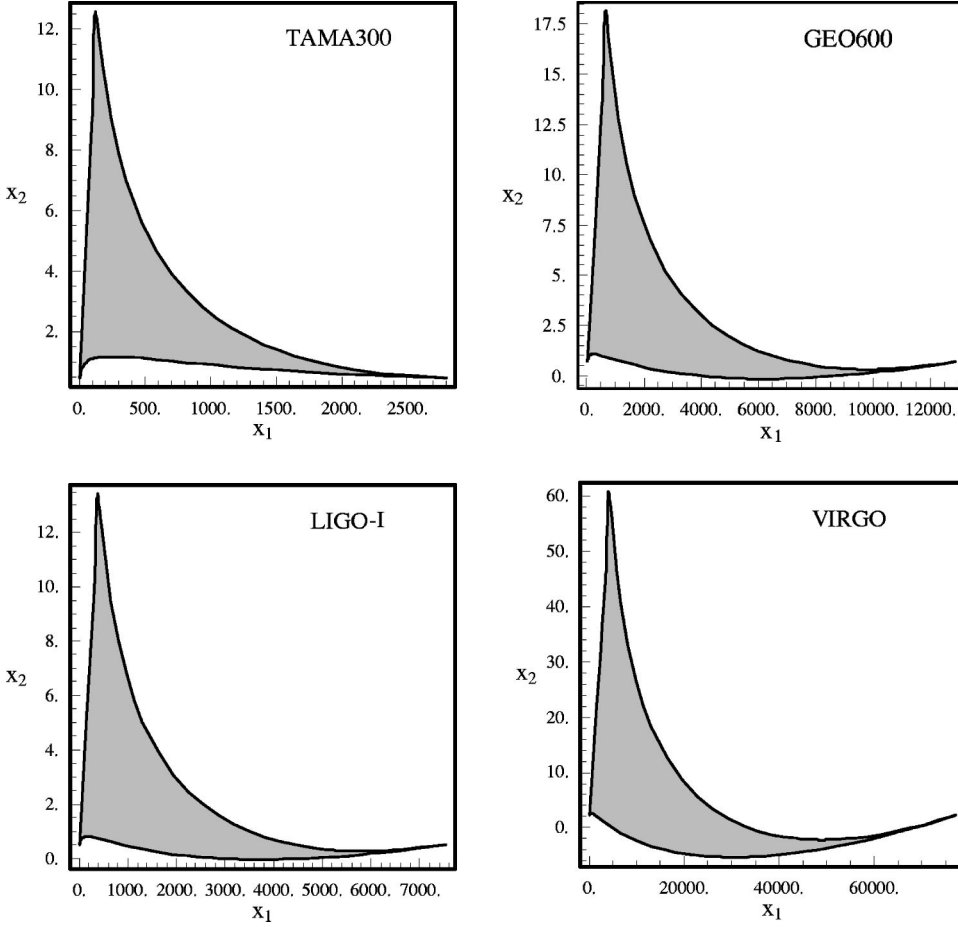| Antenna	$\Pi(f)$	Π_0 [Hz^{-1}]	f_0 [Hz]	f_i [Hz]	f_s [Hz]
TAMA300	$\frac{\Pi_0}{32}\left\{\left(\frac{f_0}{f}\right)^5 + 13\left(\frac{f_0}{f}\right) + 9\left[1 + \left(\frac{f}{f_0}\right)^2\right]\right\}$	2.4×10^{-44}	400	75	3400
GEO600	$\frac{\Pi_0}{5}\left[4\left(\frac{f_0}{f}\right)^{3/2} - 2 + 3\left(\frac{f}{f_0}\right)^2\right]$	6.6×10^{-45}	210	40	1450
LIGO-I	$\frac{\Pi_0}{3}\left[\left(\frac{f_0}{f}\right)^4 + 2\left(\frac{f}{f_0}\right)^2\right]$	4.4×10^{-46}	175	40	1300
VIRGO	$\frac{\Pi_0}{4}\left[290\left(\frac{f_i}{f}\right)^5 + 2\left(\frac{f_0}{f}\right) + 1 + \left(\frac{f}{f_0}\right)^2\right]$	1.1×10^{-45}	475	16	2750

FIG. 3. The flat simplexes $\mathcal{T}$ corresponding to $0.2M_\odot \leqslant m_1 \leqslant m_2 \leqslant 10M_\odot$ for TAMA300, GEO600, LIGO-I, and VIRGO.

LIGO-I, and VIRGO at 2PN order. Their measures (areas) are collected in Table III.

Enforcing a minimal-match constraint, in the (x_1,x_2) plane yields the *uniform* square-mesh lattice sidelength

$$\Delta = [2(1-\Gamma)]^{1/2}. \qquad (3.1)$$

The simplex area divided by Δ^2 (area spanned by each template at a given Γ) provides a close estimate of the total number of templates required, also listed in Table III for $\Gamma = 0.97$ for TAMA300, GEO600, LIGO-I, and VIRGO at 2PN order.

A. The minimal match error

Pictorial representations of the departure of $\mathcal{P}$ from $\mathcal{T}$ at order 2.5PN are shown in Fig. 4, where the simplex corresponding to $0.2M_\odot \leqslant m_1 \leqslant m_2 \leqslant 10M_\odot$ is displayed together

TABLE III. Flat simplex areas and number of templates at $\Gamma = .97$.

Antenna	Simplex area [sec^2]	No. of templates at $\Gamma = 0.97$
TAMA300	5987	9.98×10^4
GEO600	38931	6.49×10^5
LIGO-I	16842	2.81×10^5
VIRGO	546689	9.11×10^6

with its (Euclidean) distance $\delta = (x_3^2 + x_4^2 + x_5^2)^{1/2}$ from $\mathcal{P}$ as a function of x_1, x_2, for TAMA300, GEO600, LIGO-I, and VIRGO at 2PN order. The obvious question is to what extent does the shown difference spoil the minimal-match condition enforced in $\mathcal{T}$, due to the fact that the *true* wave form space is $\mathcal{P}$.

Let h be a (ν−PN) chirp signal, and let $H \equiv (x_1^{(h)}, x_2^{(h)}, \ldots, x_{2\nu+1}^{(h)})$ and $\tilde{H} \equiv (x_1^{(h)}, x_2^{(h)}, 0, \ldots, 0)$ the corresponding points in $\mathcal{P}$ and $\mathcal{T}$. By construction, $\forall\, h$ in the admissible spin-free source parameter range $m_{min} \leqslant m_1 \leqslant m_2 \leqslant m_{max}$, there will be at least one lattice node $\tilde{G} \equiv (x_1^{(g)}, x_2^{(g)}, 0, \ldots, 0) \in \mathcal{T}$ such that

$$M(\tilde{h}, \tilde{g}) = 1 - \delta_{pq}(x_p^{(\tilde{h})} - x_p^{(\tilde{g})})(x_q^{(\tilde{h})} - x_q^{(\tilde{g})}) = \Gamma, \qquad (3.2)$$

where $\tilde{h}$ and $\tilde{g}$ are the wave forms corresponding to $\tilde{H}$, $\tilde{G}$, respectively. On the other hand, from Eqs. (2.1) and (2.3),

$$M(h,g) = 1 - \gamma_{pq}(x_p^{(h)} - x_p^{(g)})(x_q^{(h)} - x_q^{(g)})$$
$$= 1 - \gamma_{pq}(x_p^{(\tilde{h})} - x_p^{(\tilde{g})})(x_q^{(\tilde{h})} - x_q^{(\tilde{g})}), \qquad (3.3)$$

where $p, q = 1, 2$, and [26]

$$\gamma_{pq} = G_{rs} \frac{\partial \theta^r}{\partial x^p} \frac{\partial \theta^s}{\partial x^q}, \qquad (3.4)$$
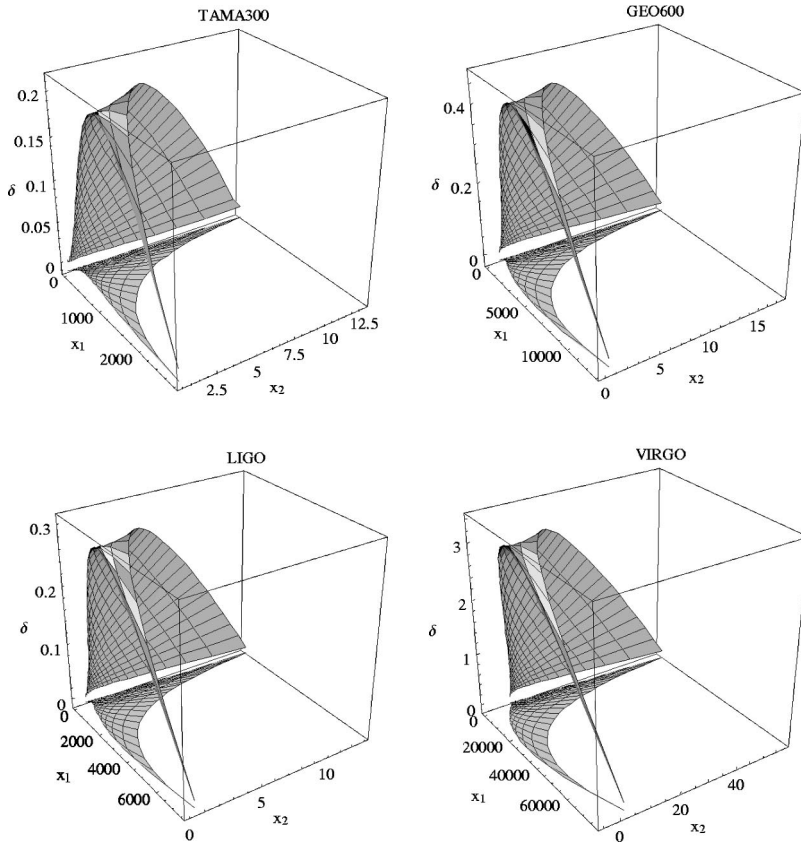
FIG. 4. The Euclidean distance $\delta=(x_3^2+x_4^2+x_5^2)^{1/2}$ between the manifolds $\mathcal{P}$ and $\mathcal{T}$ as a function of x_1, x_2 for TAMA300, GEO600, LIGO-I, and VIRGO.

where $r,s=1,2,\ldots,2\nu+1$. Let $\vec{x}\rightarrow\vec{y}$ be the (unit) rotation which diagonalizes the matrix $\gamma_{pq}-\delta_{pq}$. Then

$$|M(h,g)-M(\tilde{h},\tilde{g})|=|\eta_1(y_1^{(\tilde{h})}-y_1^{(\tilde{g})})^2+\eta_2(y_2^{(\tilde{h})}-y_2^{(\tilde{g})})^2|$$

$$\leq\max(|\eta_1|,|\eta_2|)[(y_1^{(\tilde{h})}-y_1^{(\tilde{g})})^2$$

$$+(y_2^{(\tilde{h})}-y_2^{(\tilde{g})})^2]$$

$$=\max(|\eta_1|,|\eta_2|)(1-\Gamma), \qquad (3.5)$$
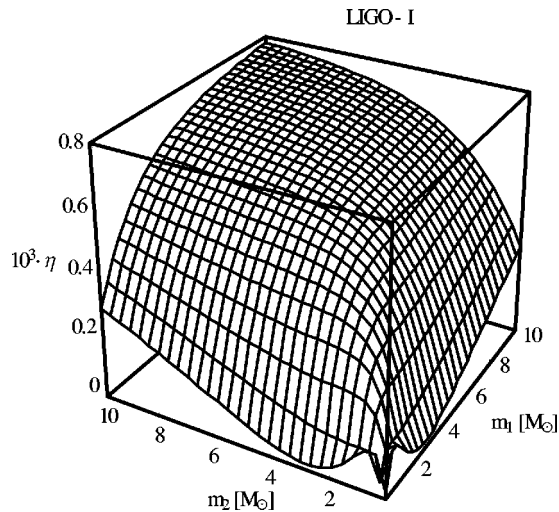
where η_1,η_2 are the eigenvalues of the matrix $\gamma_{pq}-\delta_{pq}$. The Γ-independent quantity

$$\eta=\frac{|M(h,g)-M(\tilde{h},\tilde{g})|}{1-\Gamma}=\max(|\eta_1|,|\eta_2|) \qquad (3.6)$$

is a measure of the match degradation due to using a *flattened* parameter space, and is displayed in Fig. 5 as a func-
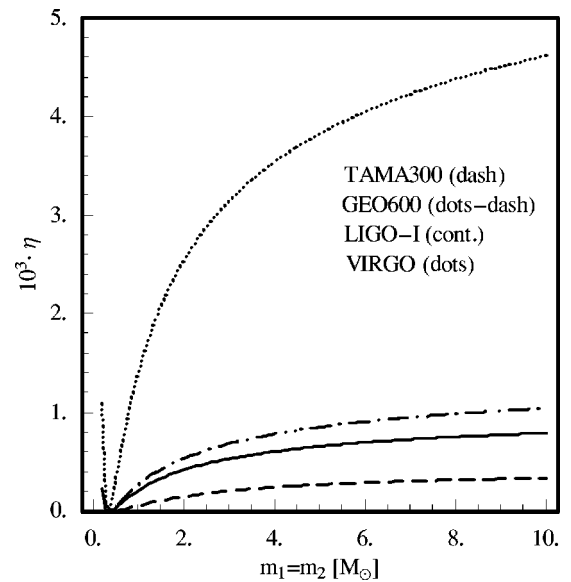

FIG. 5. The quantity η, Eq. (3.6), vs m_1, m_2 for LIGO-I.

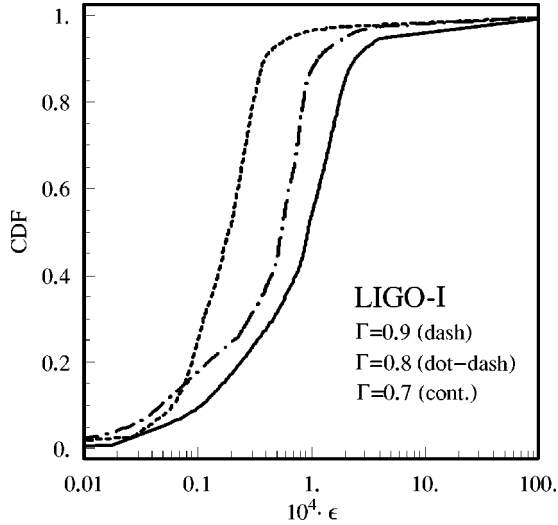FIG. 6. The quantity η, Eq. (3.6), vs $m_1=m_2$ (worst case) for TAMA300, GEO600, LIGO-I, and VIRGO.

FIG. 7. Cumulative distribution of ϵ, Eq. (3.7), for LIGO-I at $\Gamma=0.7\times$, $0.8\times$, 0.9×10^4 trial sources in $0.2M_\odot\leqslant m_1\leqslant m_2\leqslant10M_\odot$.

FIG. 8. Template density reduction vs Γ after cardinal interpolation (2PN order templates, LIGO-I).

tion of m_1, m_2 in $0.2M_\odot\leqslant m_{1,2}\leqslant10M_\odot$, for the special case of LIGO-I at 2PN order. The maximum value is attained for $m_1=m_2$. This property is common to *all* first-generation antennas quoted in Table I. In Fig. 6 the quantity η is displayed as a function of $m_1=m_2$ (worst case) for TAMA300, GEO600, LIGO-I, and VIRGO at 2PN order.

It is seen that the minimal-match condition enforced using $\mathcal{T}$ as the wave form/template parameter space is *not* spoiled significantly when the signal (and the template) belongs to $\mathcal{P}$.

The above argument might perhaps be weak at *low* values of Γ, as e.g., typically required for the initial steps of hierarchical search procedures [27], where the quadratic approximation (2.1) might be no longer accurate enough [22]. In order to evaluate the (maximum) minimal-match error under these broader conditions, we generated 10^4 random pairs (m_1,m_2), uniformly distributed in the allowed source parameter range $0.2M_\odot\leqslant m_1\leqslant m_2\leqslant10M_\odot$. For each of the above, we drew a closed-curve $\mathcal{C}\subset\mathcal{T}$ centered around the corresponding point $\tilde{F}\in\mathcal{T}$, whose points $\tilde{G}$ correspond to (all) templates $\tilde{g}$ for which $M(\tilde{h},\tilde{g})=\Gamma$, and computed

$$\epsilon=\sup_{\tilde{G}\in\mathcal{C}}\frac{|M(h,g)-M(\tilde{h},\tilde{g})|}{\Gamma}=\sup_{\tilde{G}\in\mathcal{C}}\left[1-\frac{M(h,g)}{\Gamma}\right]. \tag{3.7}$$

The cumulative distributions of ϵ, for the special case of LIGO-I at 2PN order, corresponding to $\Gamma=0.7,0.8,0.9$ are shown in Fig. 7. Not unexpectedly, the Tanaka-Tagoshi coordinates are seen to work also at relatively low values of Γ.

B. Cardinal interpolation beyond 1PN

In the obtained uniform lattice, the application of the cardinal interpolation technique introduced in Ref. [16] is straightforward. For 1PN templates this latter yields a fourfold reduction in the template density and total number at $\Gamma=.97$, as shown in Ref. [17]. A main motivation of this
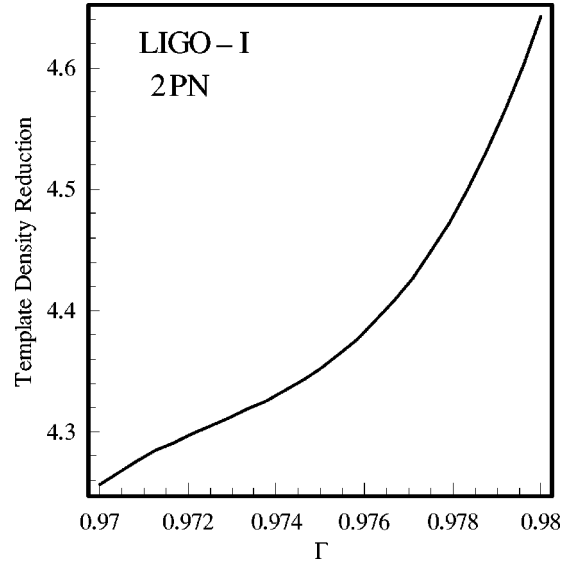
study has been to check whether a comparable reduction in the number of templates could be obtained using Tanaka-Tagoshi parametrized 2PN templates. Numerical simulations show that this is indeed the case: the 2PN template density reduction as a function of the minimal match Γ is shown in Fig. 8.

C. Computation of templates

In the following we shall denote the (linear) direct ($\vec{\theta}\rightarrow\vec{x}$) and inverse ($\vec{x}\rightarrow\vec{\theta}$) Tagoshi-Tanaka transformation operators as Ξ_{ij} and Θ^{ij}, respectively.

The template corresponding to the node $(x_{1,k},x_{2,k})$ of the (uniform) lattice in the (x_1,x_2) plane should be computed, in principle, by solving (e.g., numerically) the system

$$\Xi_{1i}\theta^i(m_{1k},m_{2k})=x_{1,k},$$

$$\Xi_{2i}\theta^i(m_{1k},m_{2k})=x_{2,k}, \tag{3.8}$$

to obtain the corresponding values m_{1k},m_{2k} of m_1,m_2, whereby *all* the θ^i functions and hence the (*exact*) template phase (1.4) can be computed. The above *exact* (and computationally expensive) procedure for computing the template phases needs *not* to be applied for *all* lattice nodes. Indeed, as noted in Ref. [20], the *change* in the θ^i between the templates at (x_1,x_2) and $(x_1+\delta x_1,x_2+\delta x_2)$ is well approximated by

$$\Delta\theta^i\approx\Theta^{i1}\delta x_1+\Theta^{i2}\delta x_2 \tag{3.9}$$

as a consequence of the fact that $x_3,x_4,\ldots,x_{2\nu+1}$ are *almost* constant throughout relatively *large* portions of the (x_1,x_2) plane. As a result, the phase *difference* between neighboring templates can be taken as *uniform* throughout *extended* regions of the (x_1,x_2) plane, which makes the template set construction relatively cheap. One can accordingly compute the exact template phases using Eq. (3.8) for a set

of *sparse* lattice nodes. The phase of templates belonging to neighborhoods of these sparse nodes can be obtained using Eq. (3.9). The *size* of the above neighborhoods (i.e., equivalently, the distance between the sparse nodes) should be chosen so as not to spoil the prescribed minimal match condition [28].

A possible natural strategy is to place the exact templates nearby the median lines of $\mathcal{T}$, starting from their common crossing point [29]. We checked by numerical simulation that a few (e.g., ~ 50 for LIGO-I at $\Gamma = 0.97$) exactly computed sparse templates are sufficient to compute all the remaining ones via Eq. (3.9), without spoiling the minimal match condition throughout the whole waveform parameter range.

IV. CONCLUSIONS

It has been shown that the Tanaka-Tagoshi coordinates are effective to set up a uniform lattice of post-1PN spin-free binary-inspiral templates under a given minimal match constraint, for all first generation interferometric antennas. This allows to extend readily the minimum redundant cardinal interpolation techniques of the correlator bank introduced by the authors to the highest available order PN templates, yielding a computational gain comparable to the 1PN case.

Several possible variations of the Tanaka-Tagoshi method can be envisaged. For instance, a 2D *simplex* is used here to approximate the parameter manifold. Using a 2D *complex* could possibly improve the accuracy. Further, the 2D simplex is obtained by point collocation, i.e., by enforcing contact between the vertices of the simplex $\mathcal{T}$ and those of the manifold $\mathcal{P}$. Other approximation philosophies could be used, including, e.g., least mean squares, etc.

APPENDIX A: THE PN WAVE FORM PARAMETER MANIFOLD

In this appendix we rephrase the well known construction of a metric in the binary-inspiral wave form parameter space, first introduced by Owen [21] and adopted by Tanaka and Tagoshi [20], using a slightly different notation. Define

$$u(h,g) = \frac{\int_{f_i}^{f_s} f^{-7/3} \exp\{j[2\pi f \Delta T_c - \Delta \phi_c + \Delta \Psi^{(\nu)}(f; \vec{\xi}_h, \vec{\xi}_g)]\} \frac{df}{\Pi(f)}}{\int_{f_i}^{f_s} f^{-7/3} \frac{df}{\Pi(f)}}, \tag{A1}$$

and let

$$\langle v(f) \rangle = \frac{\int_{f_i}^{f_s} df \frac{f^{-7/3}}{\Pi(f)} v(f)}{\int_{f_i}^{f_s} df \frac{f^{-7/3}}{\Pi(f)}}. \tag{A2}$$

It is readily proved that

$$u(h,g) = 1 + j \langle \zeta_n \rangle \Delta \theta^n - \frac{1}{2} \langle \zeta_m \zeta_n \rangle \Delta \theta^m \Delta \theta^n + \cdots, \tag{A3}$$

where $m,n = 0,1,\ldots,2\nu+1$, and

$$\zeta_0 = 2\pi(f/f_0), \quad \theta_0 = f_0 T_c. \tag{A4}$$

From Eqs. (A1)–(A4) one gets

$$\max_{\Delta \phi_c} \langle h,g \rangle = |u(h,g)| = 1 - G'_{mn} \Delta \theta^m \Delta \theta^n, \tag{A5}$$

where $m,n = 0,1,\ldots,2\nu+1$ and

$$G'_{mn} = \frac{1}{2}(\langle \zeta_m \zeta_n \rangle - \langle \zeta_m \rangle \langle \zeta_n \rangle). \tag{A6}$$

Equations (A5) and (A6) allow us to express the match as follows:

$$M(h,g) = \max_{\Delta T_c} \max_{\Delta \phi_c} \langle h,g \rangle = \max_{\Delta T_c} |u(h,g)| = 1 - G_{pq} \Delta \theta^p \Delta \theta^q, \tag{A7}$$

where now $p,q = 1,2,\ldots,2\nu+1$ and [30]

$$G_{pq} = G'_{pq} - \frac{G'_{p0} G'_{q0}}{G'_{00}}. \tag{A8}$$

APPENDIX B: CONSTRUCTING THE TANAKA-TAGOSHI COORDINATES

Let $m_{min} \leq m_1 \leq m_2 \leq m_{max}$ be the allowed mass range, and let $\vec{p}_i$, $i=1,2,3$ be the vertices of the parameter space

manifold $\mathcal{P}$ corresponding to $(m_1 = m_2 = m_{min})$, $(m_1 = m_{min}, m_2 = m_{max})$, and $(m_1 = m_2 = m_{max})$, respectively, in the $(2\nu + 1)$-dimensional PN parameter space with metric G_{pq}. The Tanaka-Tagoshi coordinates are obtained as follows. One first performs a (linear) coordinate transformation

$$\vec{\theta}\,' = \mathbf{\Lambda}^{1/2} \mathbf{P} \vec{\theta} \qquad (B1)$$

to make the new coordinates orthogonal. The required transformation is obtained from the Jordan decomposition of **G**,

$$\mathbf{G} = \mathbf{P}^T \mathbf{\Lambda} \mathbf{P}, \qquad (B2)$$

i.e., in component notation,

$$G_{pq} = P_p^{(m)} \Lambda_{mn} P_q^{(n)}, \qquad (B3)$$

where $\Lambda_{mn} = \lambda^{(n)} \delta_{mn}$, $\lambda^{(n)}$ are the eigenvalues and $P_q^{(n)}$ the eigenvectors of **G**.

Next, one seeks a rotation $\vec{x} = \mathbf{Q}\vec{\theta}\,'$ which bears (modulo a trivial translation) *all* vertices $\vec{p}_i\,'$, $i = 1,2,3$ of the manifold $\mathcal{P}$ onto the coordinate plane (x^1, x^2). The problem is thus reduced to that of finding an orthogonal matrix **Q** such that

$$\mathbf{Q}(\vec{p}_3\,' - \vec{p}_1\,') = \alpha_{11} \hat{x}_1,$$

$$\mathbf{Q}(\vec{p}_2\,' - \vec{p}_1\,') = \alpha_{21} \hat{x}_1 + \alpha_{22} \hat{x}_2, \qquad (B4)$$

where α_{11}, α_{21}, α_{22} are suitable real numbers, and $\hat{x}_i$ denote the (new, unit) basis vectors. The system (B4) does *not* have a unique solution for **Q**. However, a possible solution is readily obtained as follows. Let **Z** the matrix constructed out of the (column) vectors:

$$\vec{p}_3\,' - \vec{p}_1\,', \ \ \vec{p}_2\,' - \vec{p}_1\,', \ \ \hat{\theta}_3\,', \ldots, \hat{\theta}_{2\nu+1}\,'. \qquad (B5)$$

It is readily shown that **Z** is nonsingular. The straightforward (unique) QR decomposition of **Z**, viz. [31]

$$\mathbf{Z} = \mathbf{Q}^T \mathbf{R}, \qquad (B6)$$

where **R** is a lower triangular matrix, is obviously a solution of

$$\mathbf{Q}\mathbf{Z} = \mathbf{R}. \qquad (B7)$$

It is seen that the solution of Eq. (B7) is *also* a solution of Eq. (B4), and hence the sought **Q** in Eq. (B4) is the same as **Q** in Eq. (B6).

---

[1] See T. Damour, B.R. Iyer, and B.S. Sathyaprakash, Phys. Rev. D **63**, 044023 (2001), for an updated critical review of the subject.

[2] http://www.tamago.ac.jp

[3] http://geo600.uni.hannover.de

[4] http://www.ligo.caltech.edu

[5] http://www.virgo.infn.it

[6] C.W. Helström, *Statistical Theory of Signal Detection* (Pergamon Press, Oxford, 1968).

[7] The value of Γ translates into a *fraction* $(1 - \Gamma^3)$ of potentially observable sources which *might* be lost as an effect of template discretization. A value of $\Gamma = 0.97$ is commonly recommended.

[8] C. Cutler and E. Flanagan, Phys. Rev. D **49**, 2658 (1994).

[9] The stationary phase formula (1.3) is thoroughly discussed in T. Damour *et al.*, Phys. Rev. D **62**, 084036 (2000).

[10] The coalescency time T_c is formally defined as the time when the orbital frequency diverges to infinity. The adiabatic inspiral model, however, is only valid up to a last stable circular orbit [see A. Buonanno and T. Damour, Phys. Rev. D **59**, 084006 (1999)].

[11] L. Blanchet, T. Damour, B. Iyer, C.M. Will, and A. Wiseman, Phys. Rev. Lett. **74**, 3515 (1995).

[12] PN binary inspiral wave forms have been computed up to 2.5PN order. Efforts to include 3PN terms have not yet been completed [see e.g., L. Blanchet and G. Faye, Phys. Rev. D **63**, 062005 (2001)].

[13] Our notation differs from that used in Ref. [20]. For better readability, we include explicitly the null 0.5PN term in the PN phase expansion (1.4).

[14] T. Apostolatos, Phys. Rev. D **54**, 2421 (1996).

[15] B. Owen and B.S. Sathyaprakash, Phys. Rev. D **60**, 022002 (1999).

[16] R.P. Croce, Th. Demma, V. Pierro, and I.M. Pinto, Phys. Rev. D **62**, 124020 (2000).

[17] R.P. Croce, Th. Demma, V. Pierro, I.M. Pinto, D. Churches, and B.S. Sathyaprakash, Phys. Rev. D **62**, 121101(R) (2000).

[18] For the 1D parameter space of 0PN wave forms the natural coordinate choice is θ^1, proportional to the chirp mass, which is the only intrinsic parameter. For the 2D parameter space of 1PN wave forms, *any* linear combination of θ^1 and θ^3 will do the job, the one yielding a square-mesh lattice being the most convenient.

[19] T. Damour, B.R. Iyer, and B.S. Sathyaprakash, Phys. Rev. D **57**, 885 (1998).

[20] T. Tanaka and H. Tagoshi, Phys. Rev. D **62**, 082001 (2000).

[21] B. Owen, Phys. Rev. D **53**, 6749 (1996).

[22] The quadratic approximation (2.1) is accurate in a neighborhood of $M = 1$, e.g., for LIGO-I, for $M \gtrsim 0.95$.

[23] The spin-free phase is invariant upon exchange between m_1 and m_2.

[24] M. Spivak, *A Comprehensive Introduction to Differential Geometry* (Publish or Perish, Houston, 1990).

[25] The global flatness of a 2D Riemannian manifold $(\mathcal{P}, g)$ is gauged by its Gaussian curvature K [24]:

$$K = \frac{R_{1212}}{\det[g]},$$

where the (only component of the) Riemann tensor is

$$R_{1212} = \frac{1}{2}(2g_{12,12} - g_{11,22} - g_{22,11}) + \sum_{m,n}^{1,2} g^{mn}\{[21,m][12,n]$$
$$- [11,m][22,n]\}.$$

In the above formula, for the case of our interest, g_{pq} is given

by Eq. (2.3), and is a function of m_1, m_2; commas denote partial derivatives, and

$$[pq,r] = g_{pr,q} + g_{qr,p} - g_{pq,r}$$

are the Christoffel symbols of the first kind. It is well known that the 2D manifold $\mathcal{P}$ is flat, i.e., applicable to the plane, if $K = 0$.

[26] The partial derivatives in Eq. (3.4) are readily computed from the known partial derivatives of θ^i with respect to m_j, and the inverse of the Jacobian matrix obtained from the differential counterpart of Eq. (3.8).

[27] S.D. Mohanty, Phys. Rev. D **57**, 630 (1998).

[28] The *exact* change in the θ^i between a template at (x_1, x_2) and a template at $(x_1 + \delta x_1, x_2 + \delta x_2)$ is given (to first order) by

$$\Delta\theta^i_{exact} = \frac{\partial\theta^i}{\partial m_r}\frac{\partial m_r}{\partial x_p}\delta x_p.$$

The radius R of the circular neighborhood of (x_1, x_2) where the approximation (3.9) does not spoil significantly the prescribed minimal-match condition can be estimated by requir-

ing that the *mismatch* between the *exact* and *approximate* template computed at $(x_1 + \delta x_1, x_2 + \delta x_2)$ using Eq. (3.9) be, e.g., one order of magnitude smaller than $1 - \Gamma$, viz.

$$\Gamma^{pq}\delta x_p \delta x_q \leqslant \frac{1 - \Gamma}{10},$$

where

$$\Gamma^{pq} = G_{rs}\left[\frac{\partial\theta^r}{\partial m_h}\frac{\partial m_h}{\partial x_p} - \Theta^{rp}\right]\left[\frac{\partial\theta^s}{\partial m_k}\frac{\partial m_k}{\partial x_q} - \Theta^{sq}\right]$$

and all partial derivatives are evaluated at (x_1, x_2). This gives an asymptotic estimate of R based on the quadratic match approximation valid for $\Gamma \approx 1$.

[29] The median lines here are (more or less arbitrarily) defined as those of the straight-edge triangle in (x_1, x_2) whose vertices coincide with those of $\mathcal{T}$.

[30] Equation (A8) is readily obtained [21] by projecting the metric on the subspace orthogonal to $\Delta\theta^0$.

[31] W.H. Press, B.P. Flannery, S.A. Teukolsky, and W.T. Vetterling, *Numerical Recipes* (Cambridge University Press, Cambridge, UK, 1992).